iJRASET
International Journal For Research in Applied Science and Engineering Technology

INTERNATIONAL JOURNAL FOR RESEARCH

IN APPLIED SCIENCE & ENGINEERING TECHNOLOGY

Volume: 5 **Issue:** V **Month of publication:** May 2017

DOI:

www.ijraset.com

Call: 08813907089 | E-mail ID: ijraset@gmail.com

Volume 5 Issue V, May 2017
ISSN: 2321-9653
International Journal for Research in Applied Science & Engineering Technology (IJRASET)

Numerical and Experimental Evaluation of Steel-Polymer Perforated Shear Walls

Mohammad Hooshmand[1], Shima Naji[2]
MA Graduate in Structural Engineering, Islamic Azad University, Tabriz Branch, Tabriz, Iran

Abstract: ***This article tries to numerically and experimentally investigate the behavior of perforated composite shear walls (Perforated-CSSW). For this purpose, a specific number of experimental samples have been subjected to loading processes under existing regulations and rules.***
According to their aspect ratios, samples have been divided into two groups of width to height ratio of 1.33 and 0.85. The first group (As-1.33) includes four samples with dimensions of 800 by 600 millimeters. One of these samples is selected as the reference non-fiber containing sample while the rest of the samples had been reinforced with Carbon Fibers. The entire samples of this group had 24 holes or circular openings sorted on the infill plate of the shear wall.
After determination of a suitable loading protocol, the samples were subjected to a reciprocating loading and afterwards, hysteresis curve belonging to each sample was extracted. Results yielded from hysteresis curves of each sample are compared with other samples' and investigated thoroughly.
In addition, numerical investigations have been applied along with experimental analyses. For this purpose, the aforementioned samples were modeled by the ABAQUS software. Ultimately, results obtained from numerical analyses have been compared with those obtained from experimental analyses.
Keywords: shear wall, fibers, hysteresis curve

I. INTRODUCTION

Shear walls are considered as a suitable system for resistance against lateral loads of wind and earthquake. As a result of high resistance, significant stiffness, stable hysteresis curves and suitable energy absorption, these systems have been extensively considered and made use of.

A steel shear wall includes VBEs and HBEs and an infill plate. According to the type of used steel, the structure and shape of the infill plate can be different. For example, the steel plate may be made of ordinary steel or fine building steel. Steel shear walls should be designed in a way that while creating a thorough yield for the infill plate, they also maintain the flexibility of the surrounding frame. In addition, for a better performance, the LYS steel type which is of a lower yield tension can be made use of. In terms of structure and shape of the infill plate, it can be said that this plate can be along with stiffeners or lack of them; can be composite with concrete layers or polymer fibers, can be filled or can include several openings or perforations. Most of primary studies in the early 1980s included the consideration for buckling outside the plate. In order to avoid the buckling of steel plate, this system has been designed with several different stiffeners. However, considering all the research performed on shear walls with thin plates and no stiffeners, it has been manifested that the fineness of post-buckling resistance of these systems can be highly considerable. According to previous studies (Thornburg et al. 1983[14]; Timler et al. 1983[15]; Tromposch et al. 1987[11]; Roberts et al. 1992[12][13]; Cassese et al. 1993[18]; Elgaaly et al. 1996[7]; driver et al. 1998[12]; Rezaei, 1999; Lubell et al. 2000; Berman et al. 2003[8]), the Canadian society of CAN/CSA S16-01 has specified certain regulations for designing steel shear walls which allows buckling and extension of tensile area in steel plates. A bold characteristic for unstiffened steel shear walls is their considerable post-buckling resistance and the resultant creation of tension area. In other words, when a steel shear wall is exposed to lateral loading, the infill plate's center is exposed to the effect of pure shear and therefore a 45 degrees angle is created between main tensions and the line of loading. Therefore, main tensions are imposed on the system in both forms of compressive and tensile stresses. Since this is a high angle for conventional SPSWs, consequently the overall buckling resistance of the steel plate would be insufficient. As a result, when the system is subjected to a lateral load, the plate starts to buckle as a result of dominance of main compressive tensions over compressive strength of the system. From this point on, and since the buckling lines are perpendicular to main compressive tension, the task of load transfer is the duty of main tensions in plate. This post-buckling event is referred to as Tension Field.

Since the very beginning of emergence of unstiffened shear walls, researchers have shown a great deal of interest in behavior of this

Volume 5 Issue V, May 2017
ISSN: 2321-9653
International Journal for Research in Applied Science & Engineering Technology (IJRASET)

system under different conditions. Some of these conditions include different types of loading; using perforations and special stiffeners, different composite systems with different material and etc. Some of the previous works in this field are mentioned in following section. Recently, several researches have been performed regarding improvement of behavior of the SPSWs. The point of start of these researches is the work of Bruneau et al. (2005) aimed at using perforations as openings for crossing facilities and creation of the Design level required amount of resistance and stiffness when using thin plates is impossible. In other words, creating sorted openings or perforations on thick plates, the levels of stiffness and resistance can be controlled and reduced to suitably fit the design level requirements.

On the other hand, several researchers have also investigated various composite systems for improvement of behavior of SPSWs and reinforcing them. Among these researches it can be pointed to the studies guided by Zhao et al. in years of 2004 and 2007 for steel plates combined with layers of armed concrete. Other researches in this field include the researches performed by Hatami et al. (2010) and Alipour Tabrizi (2011) on steel plates reinforced with Polymer fibers. Considering the literature of the subject matter, it can be concluded that currently no researches have been performed on Composite steel shear walls with plaid perforations or reinforcement of SPSWs with plaid perforations. On the other hand, it should be mentioned that this type of SPSW has only been investigated by Bruneau et al. on this basis and considering the limited amount of researches on the aforementioned system; the focus of this article is on the system of SPSW with matrix or plaid perforations (openings) and reinforcement of the latter with the emerging Polymeric materials.

II. METHODS

Determination of dimensions and manner of implementation of system

The section 17.2b of the AISC 341 [6] regulation has been referred to for selecting suitable dimensions for samples. In this reference, it has been determined that the aspect ratios must be according to the following limitation:

$$0.8 < L / h \leq 2.5$$

For further investigation of the aforementioned system, the experimental samples were divided into two groups with different aspect ratios in a way that both aspect ratios of larger and smaller than one were included. For the first group, the aspect ratio of 600 by 800 millimeters is determined. As you can see the L/H is equal to 1.33 which satisfies the aforementioned limitation. For the second group, an aspect ratio of 0.85 and dimensions of 600mm (width) by 700mm are selected. As you can see, here the L/H ratio is 0.85 which also satisfies the upper limitation. In order to maintain the tensile strength after removing the bonding between steel plate and polymer fibers, the section of the external frame or beams and columns are selected in a way that the aforementioned section holds the composite plate within itself. In other words, since in this condition the steel plate and polymer fibers are thoroughly connected to the frame, the fibers will not be detached from the system after removing the bonding. As long as the fibers are not detached, they will continue maintaining their tensile strength. As a result, two UNP profiles are used for beam and column sections. These Profiles create an "I" shaped section and the composite plate is placed between these profiles. In addition, the attachment of profiles and the plate is done through bolts embedded in profiles. It is worth mentioning that arc welding was used for attachment of beams to columns. Figure (1) and figure (2) respectively show the images of primary designs for the As-1.33 and As-0.85 groups. These images show the order of perforations and the manner of attachment of the plate to beams and columns. The circular perforations of openings have a diameter of 51 millimeters and also the vertical and horizontal space between perforations is equal to 80 millimeters.

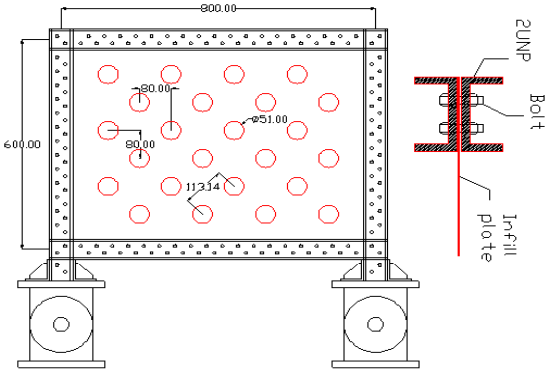

Figure (1): The Schematic For Samples Belonging To The As-1.33 Group

Volume 5 Issue V, May 2017
ISSN: 2321-9653
International Journal for Research in Applied Science & Engineering Technology (IJRASET)

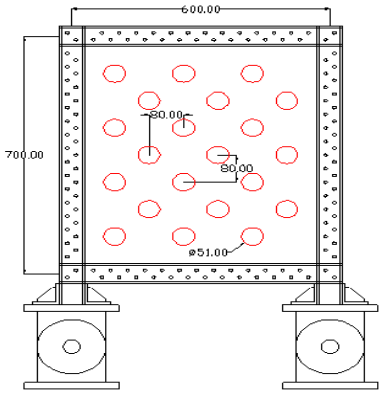

Figure (2): the schematic for samples belonging to the As-0.85 group

A. Designing the experimental samples of As-1.33 group

1) Primary design: Since designing a steel shear wall requires the calculation of the coefficient of Tension Field of alpha and calculation of this coefficient requires the sections of beams and columns; primarily a certain thickness was assumed for the steel plate and afterwards, with respect to limitations cited in various regulations, the sections of beams and columns were calculated. We suppose that plate thickness is equal to 0.4mm. The relation (3-1) shows the moment of inertia of columns specified by section 17.4g of the AISC341. In addition, certain limitations for columns considered by AISC-Steel Design Guide 20 [4] have been provided in relation (3-2).

(1-3) $$I_c \geq 0.00307 \frac{t_w h^4}{L}$$

(3-2) $$I_b \geq 0.003 \frac{\Delta t_w L^4}{h}$$

"H" is the center to center space between beams and L is the center to center space between columns. In addition Δt_w is the difference between thicknesses of plates in two consecutive layers.

$$0.00307 \frac{t_w h^4}{L} = 0.00307 \times \frac{0.04 \times 60^4}{80} = 20 cm^4 \qquad I_c \geq 20 cm^4$$

$$0.003 \times \frac{\Delta t_w L^4}{h} = 0.003 \times \frac{0.04 \times 80^4}{60} = 82 cm^4 \qquad I_b \geq 82 cm^4$$

With a little compensation, we use the 2UNP60 for both beams and columns. Afterwards, we make use of the relation (3-3) suggested by Thorburn in order to calculate the tension field angle:

(3-3) $$\tan^4 \alpha = \frac{1 + t_w L \left[\frac{1}{2 A_c} + \frac{L^3}{120 I_b h} \right]}{1 + t_w h \left[\frac{1}{A_b} + \frac{h^3}{360 I_c L} \right]}$$

The A_B and A_c are the sections of beams and columns. We have:

$$tg^4 \alpha = \frac{1 + 0.04 \times 80 \left[\frac{1}{2 \times 13} + \frac{80^3}{120 \times 63.2 \times 60} \right]}{1 + 0.04 \times 60 \left[\frac{1}{13} + \frac{60^3}{360 \times 63.2 \times 80} \right]} = \frac{4.72}{1.47} \Rightarrow \alpha = 53.2^0$$

It is worth mentioning that existence of several openings on the plate have resulted in disruption of main tensile stresses and

Volume 5 Issue V, May 2017
ISSN: 2321-9653
International Journal for Research in Applied Science & Engineering Technology (IJRASET)

therefore the tension field angle is no longer universally equal throughout the plate. However, the rest of calculations are performed considering the same previously calculated amount of alpha.

B. Designing the experimental samples of As-0.85 group

A reason for dividing the samples into two groups of As-1.33 and As-0.85 was comparison of behavior of the system under different plate sizes. In order to make comparisons equally, the exact same sections used for designing the As-1.33 samples are used for the As-0.85 group. In other words, beams and columns are again consisted of 2UNP60 and the thickness of the selected plate is also 0.4.

1) *Column joints:* Each of the joints is able to carry more than 8 tons of tensile and compressive loads. Steel plates with thickness of 2 CM and an axis with diameter of 4 CM made of ST52 steel.
2) *Controlling the loading capacity of samples:* In this section, the controlling of loading capacity of samples is only done for the As-1.33 group. For this purpose, the relations stated in research performed by Vian et al. [21] have been used. In addition the reduced loading coefficient as a result of existence of perforations is calculated according to the research performed by Purba [20]. Figure (3): details of As-1.33 group

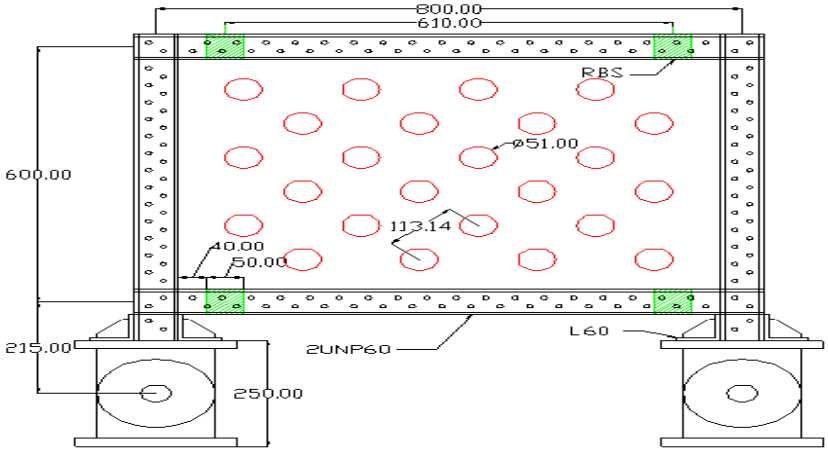

Figure (3) shows the entire details of the samples belonging to the As-1.33 group. The dimensions and sizes shown in this figure are used for calculation of capacity control.

The total system capacity is obtained through addition of the capacity of the frame to the shearing capacity of the infill plate. First, the Frame's capacity is calculated through the following relation:

(3-45) $$V_f = \frac{4\beta M_p}{\lambda(h + h_{hinge})}$$

In the upper relation, M_P is the beam anchor; beta is the ratio of plasticity module to plasticity of the entire beam section. Landau is the ratio of center to center space between RBSs to frame width and H_{inge} is the space between the center of the hinge and beam X.

(3-46) $$M_p = Z_x . F_y$$
$$M_p = (23)(2400 \times 1.1) \rightarrow M_p = 60720 \quad kg.cm$$
$$\lambda = \frac{L_h}{L} \rightarrow \lambda = \frac{61}{80} \rightarrow \lambda = 0.76$$

In order to consider for material over-strength, the value of F_Y is multiplied by 1.1.
The value of beta is considered as 2.3 again.

$$V_f = \frac{4(2/3)(60720)}{0.76(60 + 21.5)} \rightarrow V_f = 2614\ kg$$

The capacity of steel plates with no openings or perforations is calculated through the following relation:

(3-47) $$V_p = \frac{1}{2} F_y t_w \sin 2\alpha$$

In this section, the alpha value of 45 degrees is considered for guaranteeing the result

Volume 5 Issue V, May 2017
ISSN: 2321-9653
International Journal for Research in Applied Science & Engineering Technology (IJRASET)

$$V_p = (0.5)(1900)(0.04)(80)\sin(2\times 45) = 3040\,kg$$

As a result of existence of column joints, the upper value is reformed in the following way:

(3-48) $$V'_p = \frac{h}{(h + h_{hinge})}.V_p$$

$$V'_p = \frac{60}{(60 + 21.5)}.(3040) \rightarrow V'_p = 2238\ kg$$

Afterwards, the coefficient of capacity reduction is applied:

(49-3) $$V''_{p(perf)} = V'_p\,(1 - 0.7\frac{D}{S_{dia}})$$

$$V''_{p(perf)} = 2238 \times (1 - 0.7\frac{51}{113}) \rightarrow V''_{p(perf)} = 1513\ kg$$

The total system loading capacity will be equal to:

(50-3) $$V_{total} = V_f + V''_{p(perf)}$$

$$V_{total} = 2614 + 1531 \approx 4ton < 8ton\ o.k$$

In this section, we have tried to design a suitable system for manufacturing samples in a way that the maximum tensile strength of CRF fibers is utilized. In this system even if the fibers are detached from the steel plate, they will still maintain their tensile strength as a result of being attached to the surrounding frame from four sides. In addition, UNP profiles have been used for beam and column elements. In this regard, the UNP profiles are attached to each other in a consecutive order and the composite plate is placed between the 2UNP profiles. Afterwards, the entire complex is attached through bolts embedded on the profiles. With respect to the aforementioned limitation cited in AISC341 regulatory, arbitrary dimensions have been selected for samples in a way that the samples are readily divided into two groups with aspect ratios of 1.33 as the As-1.33 group, and the aspect ratio of 0.85 as the As-0.85 group. The dimensions of the former are 600x800 millimeters and the latters' dimensions are 600x700 millimeters. In addition, considering the types of commercially available steel plates, a thickness of 0.4 was selected for the infill plate. Further, with respect to cited limitations for beams and columns, a profile was selected for the aforementioned elements namely as the "primary design". Afterwards, the profiles were tested for validity. After calculations, it was concluded to make use of 2UNP60 profiles. These profiles are attached to each other and the steel plate through highly strong bolts with a space of 2.5 centimeters between each bolt. It is worth mentioning that arc welding was used in order to attach beams to columns. The theoretically calculated capacity for such a system is equal to 4 tons. As it was mentioned, the experimental samples included two groups of As-1.33 and As-0.85. The first group included 4 samples and the second, included 3 samples. In each group, one sample is the reference non-polymer-containing sample. Clearly, the rest of the samples are composites that only differ in number of layers of fibers and orientation of fibers. Displacement assessment devices have been used for measurement of displacement of sample or buckling of the infill plate. Furthermore, a strain meter was used for measurement of infill plates' strain. In terms of installation of samples, firstly they are attached to the column joint that is already attached to the floor of the laboratory. Afterwards, the sample is attached to the load-cell, jack and the jack's support. In addition, a pair of lateral inhibitors was used in order to keep the wall moving in only one direction. Figure 4 shows the complete set of a sample ready for testing.

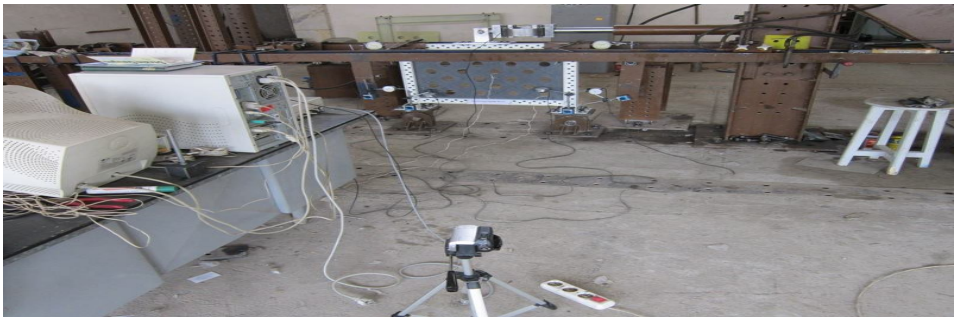

Figure (4), an image of a sample ready to be tested, along with required laboratory equipment

Volume 5 Issue V, May 2017
ISSN: 2321-9653
International Journal for Research in Applied Science & Engineering Technology (IJRASET)

III. RESULTS

Samples of the As-0.85 group

Sample SPSW-0.85

Figure five shows the images of tension meter at maximum displacement for both stiffness states. In this image, it can be clearly seen that the infill plate and RBSs have failed.

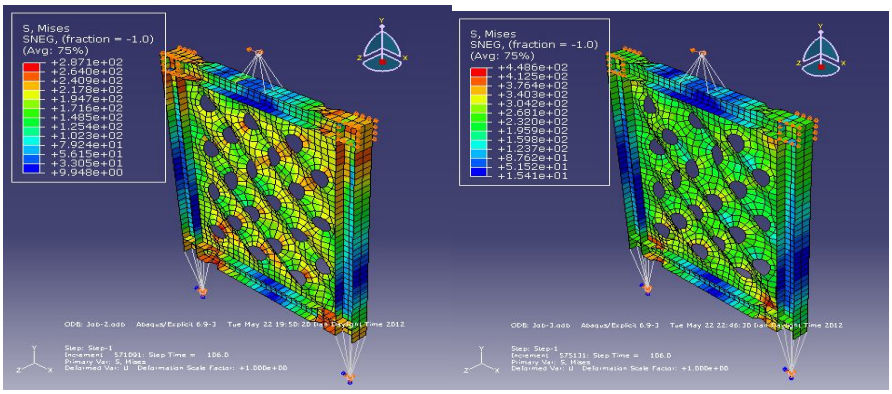

Figure (5), structure's tension meter and deformation in two stiffness states of Kinematic and Combined

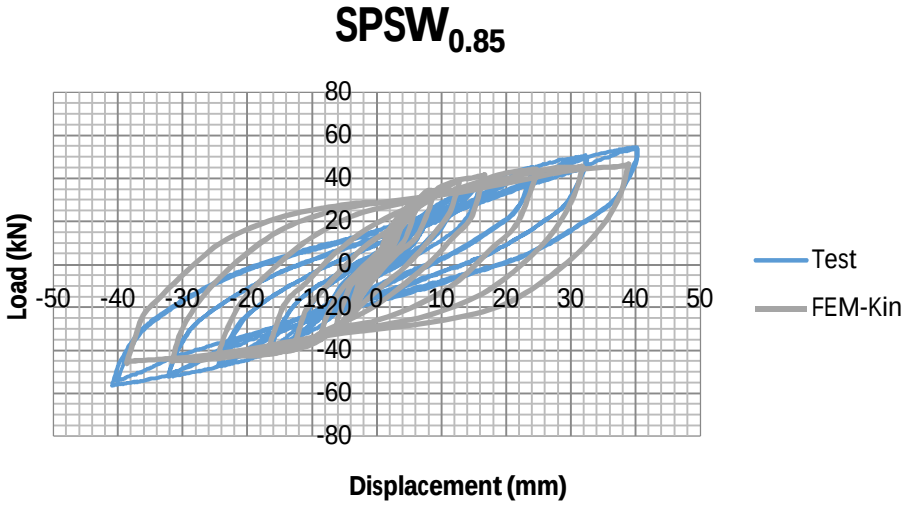

Figure (6), hysteresis curve of sample SPSW-0.85 in kinematic stiffness state and comparison of the result with experimental result

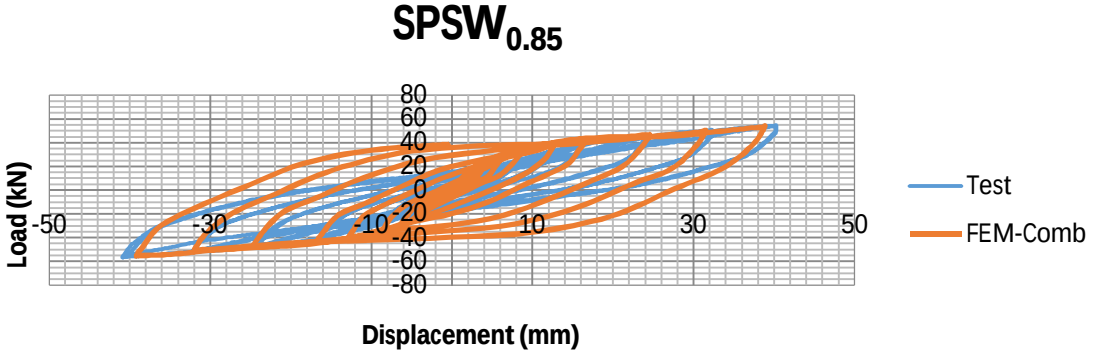

Figure (7), hysteresis curve of sample SPSW-0.85 in combined stiffness state and comparison of the result with experimental result

Extracted hysteresis curves in stiffness states of kinematic and combined are shown in figures 6 and 7. The elastic stiffness extracted from the hysteresis curve of each state is equal to 4.6kN/mm. this value is 23% higher than the value obtained for the experimental sample. As it has been shown in the images; the combined stiffness state works better than the kinematic stiffness state in terms of

Volume 5 Issue V, May 2017
ISSN: 2321-9653
International Journal for Research in Applied Science & Engineering Technology (IJRASET)

anticipation of the hysteresis curve. Maximum bearing capacity of the sample in kinematic mode is 46kN which is 15% less than the value obtained for the experimental sample. This is while the maximum capacity obtained for the stiffness mode of combined, is equal to 54kN which is consistent with the experimental samples' obtained value.

Sample CSSW-(+)-0.85

Deformation and tension meter for this sample in terms of maximum displacement can be seen in image 32-6. This image is related to the combined stiffness state.

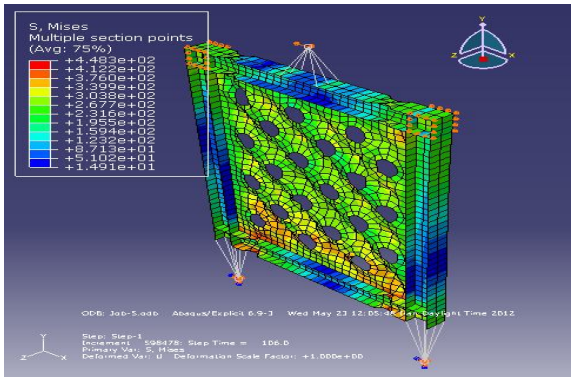

Figure (8), deformation and tension meter for the CSSW-(+)-0.85 samples in maximum displacement and under combined stiffness

In addition, the hysteresis curves of kinematic and combined stiffness states can be observed in images 7 and 8. As we have seen before, these curves also show that the system has a more anticipation power under combined stiffness mode. As a result, the final anticipation obtained from the finite element analysis method under combined stiffness method will be as it is shown in figure 9.

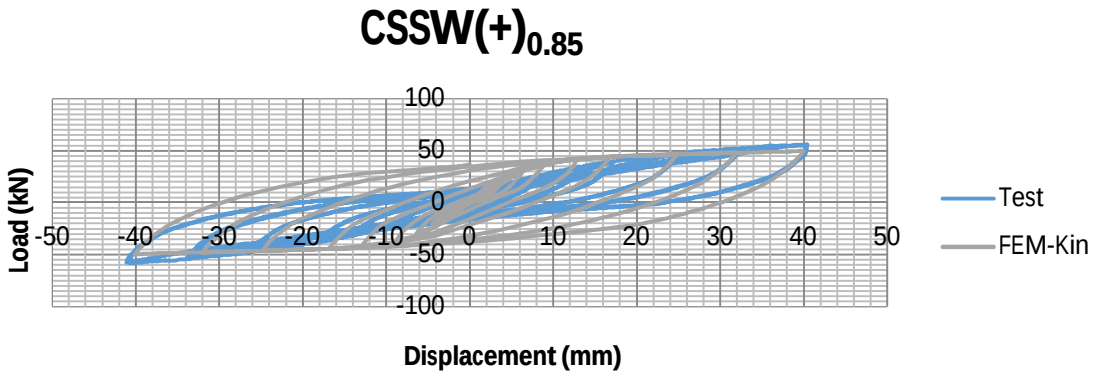

Figure (9), hysteresis curve for the CSSW-(+)-0.85 samples in kinematic stiffness mode and comparison of the result with experimental result

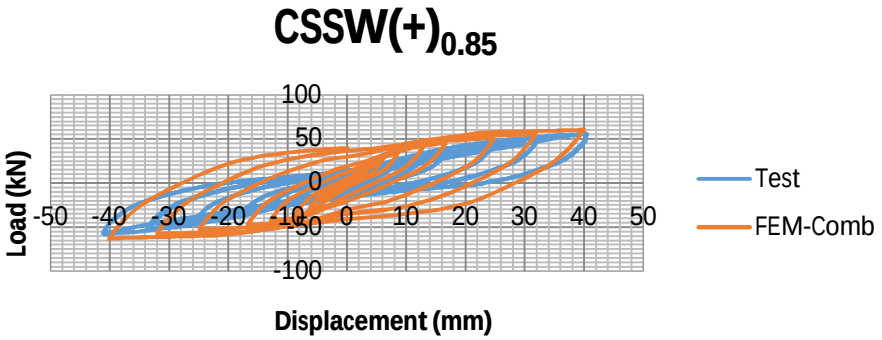

Figure (10), hysteresis curve for the CSSW-(+)-0.85 samples in combined stiffness mode and comparison of the result with experimental result

Volume 5 Issue V, May 2017
ISSN: 2321-9653
International Journal for Research in Applied Science & Engineering Technology (IJRASET)

In both stiffness states, the elastic stiffness related to finite element analysis was remained constant and equal to 5.6kN/mm. in comparison with the experimental sample, it can be seen that the aforementioned value is 35% higher. According to the upper images, the maximum bearing capacity in kinematic and combined stiffness states is respectively equal to 50kN and 61kN. Considering the aforementioned figures and images, it can be concluded that anticipation of the hysteresis curve is done better in combined mode compared to the kinematic state. However, considering the sides of the hysteresis curve shown in figure (11), it can be seen that the software shows a symmetrical situation for the sample with (+) shaped fibers. In addition it can be concluded that the lack of symmetry between hysteresis curve of the experimental sample and the orientation of aforementioned fibers cannot be anticipated by the finite elements analysis method.

Sample CSSW-(x)-0.85

Deformation and tension meter under combined stiffness mode and under maximum displacement are shown in figure 12. In this figure, the hysteresis curve of the finite element sample and comparison of the former with the curve obtained for the experimental sample can be seen. According to this image, the finite element analysis is well capable of anticipation of displacement of polymer fibers. The elastic stiffness obtained through the finite element analysis is equal to 5.6kN/mm which is larger than the elastic stiffness calculated for the experimental sample. In addition the maximum bearing capacity of the finite element analysis is equal to 71kN which is 9.5% higher than the maximum bearing capacity value obtained for the experimental sample.

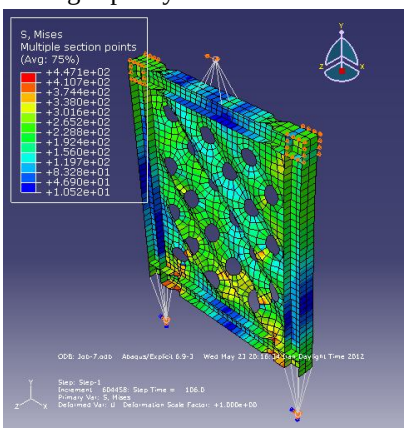

Figure (11): deformation and tension meter for the sample CSSW-(x)-0.85 under maximum lateral displacement and combined stiffness mode

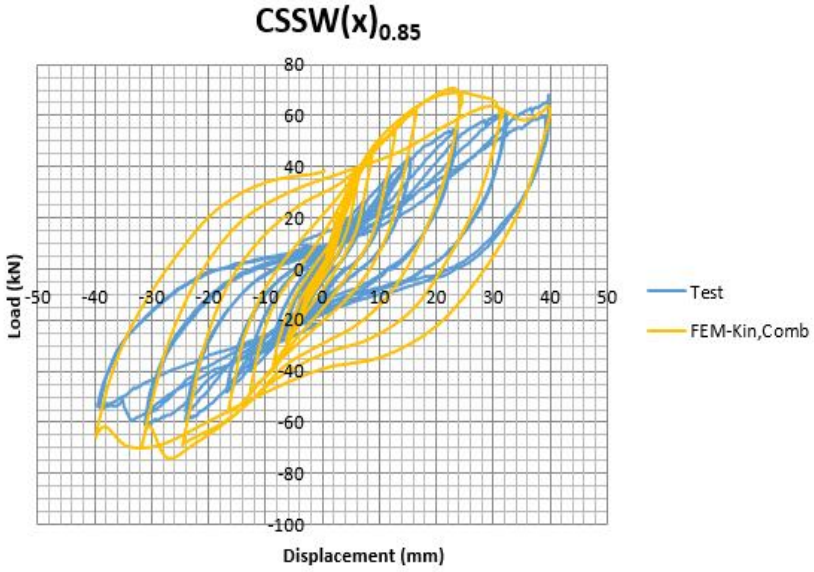

Figure (11): hysteresis curve of the CSSW-(x)-0.85 samples for both states of stiffness

Volume 5 Issue V, May 2017
ISSN: 2321-9653
International Journal for Research in Applied Science & Engineering Technology (IJRASET)

IV. CONCLUDE

In this section we have described how the modeling of a semi-static analysis is done. After modeling, the samples have been subjected to cyclic loading by the S4R element in order to extract the hysteresis curves for each sample of the finite element analysis. We have mostly referred to two notions of elastic stiffness and maximum bearing capacity for comparisons. It is worth mentioning that most of previous studies have only elaborated on kinematic stiffness modes. In fact the phenomenon of cyclic hardening cannot be introduced into the kinematic stiffness mode. Therefore, we have made efforts to separately measure both stiffness states of kinematic and combined and we have concluded that the stiffness state of kinematic works better than kinematic state in terms of anticipation of hysteresis curves. In addition it should be mentioned that since the experiment scale is very small compared to real projects, it is very difficult to fully attach the beams to columns. This is while the system defined in the finite element analysis is a merged and integrated system. Considering these content, the difference in pinching of hysteresis curves of experimental and Finite Element Software samples seems normal and expected.

V. CONCLUSION

The obtained value of cutting strength for the SPSW-1.3 sample is equal to 4 tons. In comparison with the maximum bearing capacity of the experimental sample, this value is 33% smaller. Sounds of buckling and post-buckling events in the reference sample of the As-1.33 group are normally continued until the system reaches a displacement equal to 20 to 34% of the maximum displacement of sample in each course. In addition it is worth mentioning that loudest buckling sounds are heard at 10% of maximum displacement of sample. The strain level of the channel-1 is higher than the overall strain value obtained for channel-0 in terms of the SPSW-1.3 samples. Since in perforated steel shear walls tension is focused on edges of perforations, the angle of tension field does not follow any certain or specific relations. No buckling sound was heard while testing the CSSW-(-)-1.3 sample. If horizontal fibers are attached to the As-1.33 samples, the overall elastic stiffness, maximum bearing capacity and the surface surrounded by the hysteresis curve may improve significantly, however; ductility is reduced. Still the aforementioned increase and decrease values are negligible and it can be concluded that for the As-1.33 samples, use of horizontal fibers will not result in much effect and the system works similar to the reference sample. Using CFRP fibers resulted in 50% reduction of buckling related deformations compared to the reference sample. In addition, no significant buckling related sounds were heard while testing the CSSW-(+)-1.3 samples. In addition the aforementioned composite plate remained intact and non-deformed until the end of test. In composite samples, detachment of polymer fibers from the infill plate has not resulted in any significant drops in hysteresis curves. The reason for this lies in the manner of attachment of the polymer fibers to the infill plate and the surrounding frame. Adding fibers in vertical and horizontal orientations results in disruption of symmetry of the hysteresis curve in a way that the maximum bearing capacity of the CSSW-(+)-1.3 in positive displacements is less than its bearing capacity under negative displacements. Furthermore, it was revealed that existence of horizontal and vertical fibers in CSSW-(+)-1.3 has resulted in increase of parameters such as elastic stiffness and maximum bearing capacity and the area of the surface surrounded by the hysteresis curve. This is while formability adopts different values as a result of lack of symmetry between sides of the hysteresis curve. In this regard, compared to the reference model, an increased level of deformation is observed on the side under tension and in terms of the other side, less deformation compared to the reference sample is observed. In addition existence of these fibers in the aforementioned sample result in lack of synchronization between buckling waves created on the infill plate in a way that in channels 0 and 1, the strain values have no regular or ordered pattern. In addition to these, the aforementioned vertical and horizontal fibers in CSSW-(+)-1.3 samples reduce the buckling related deformation of channel-2 up to 32%. For the CSSW-(x)-1.3 and unlike all other experimental samples of the As-1.3 group except for the reference sample; buckling sounds were heard from the very beginning point of test. After tearing of fibers in CSSW-(x)-1.3 samples, the hysteresis curve of this sample experiences a significant drop in a way that at the moment of fraction, the bearing capacity of the system rapidly decreases and reaches the bearing capacity of the reference sample. Unlike other samples, the x shape fibers for the As-1.33samples have resulted in significant increases in values of elastic stiffness, maximum bearing capacity and the area of the surface surrounded by the hysteresis curve. In addition the system undergoes a significantly reduced deformation. In terms of the CSSW-(x)-1.3, the steel plate fails in channel-0 area faster than channel-1 area. In addition it should be mentioned that existence of x shaped fibers has resulted in increased similarity between the strain values obtained for each channel. Unlike expectations, existence of x shaped fibers in CSSW-(x)-1.3 samples not only doesn't result in reduction of deformation in channel-2 area, but also this sample's depth of buckling is higher than the reference sample's. Sounds of buckling and post-buckling events in the reference sample of the As-0.85 group are normally continued until the system reaches a displacement equal to 20 to 34% of the maximum displacement of sample in each course. Unlike the SPSW-1.3 samples, the SPSW-0.85 samples'

channel-1 strain values were higher than channel-0 values. This difference continued to grow until the end of the experiment. Nonetheless, no buckling related sound is heard while testing the CSSW-(+)-0.85 sample and the fibers remained intact until the end of the experiment. Nevertheless, the hysteresis curve obtained for the CSSW-(+)-0.85 samples was not symmetrical. Adding vertical and horizontal fibers to CSSW-(+)-0.85 samples resulted in increased maximum bearing capacity, increased elastic stiffness and increased area under surrounding of the hysteresis curve. Existence of plus shaped (+) fibers in CSSW-(+)-0.85 samples resulted in decreased buckling wave depth in channel-2 area. This reduction is normally amounted as 50%. Buckling sounds are heard from the very beginning point of testing the CSSW-(x)-0.85 samples. At the end of the test it was revealed that fibers are torn on the center of the sample and close to the channel-1 area. As the fibers are torn, the hysteresis curve of the CSSW-(x)-0.85 samples experience a major drop in bearing capacity. Existence of x shaped fibers in CSSW-(x)-0.85 samples results in increase of values of maximum bearing capacity and elastic stiffness and the area surrounded by the hysteresis curve. However they result in decreased ductility compared to the reference sample. In terms of the CSSW-(x)-0.85 samples, the steel plate starts to buckle in channel-1 area sooner than the channel-0 area. In addition it was revealed that the buckling depth of the CSSW-(x)-0.85 samples in channel-2 areas is less than buckling depth of the reference sample in a way that this reduction amounts up to 24% just prior to being detached. Table 1-7 compares the composite samples of the aforementioned two groups. In this table it the individual effect of existence of cross and plus shaped fibers is shown for each sample type. In cases in which samples from both groups are marked under a sample title, it is clear that a similar effect is observed for both groups.

Table 1, comparison of performance of fibers with different orientations

Composite sample	Group name	Elastic stiffness	Maximum bearing capacity	ductility	Area of the surface surrounded by the hysteresis curve
CSSW(+)	As-1.33		●		●
	As-0.85	●	●	●	●
CSSW(×)	As-1.33	●			●
	As-0.85		●	●	

In terms of finite elements analysis, the hysteresis curve of the structure is better anticipated under combined stiffness mode which is a combination of isotropic and kinematic stiffness modes. The pinching observed in the hysteresis curve is generally resulted from the surrounding frame and its joints. Since the selected samples of this article of a small size compared to the real projects, attachment of beams to columns has been difficult and therefore, this pinching is considered normal. However, in terms of Software based modeling, a merged and integrated system is defined for the software which may not have a suitable anticipation for pinching.

REFERENCES

[1] AISC, ANSI/AISC 341-05. Seismic Provisions for Structural Steel Buildings. American Institute of Steel Construction, Chicago (IL).
[2] AISC, ANSI/AISC 358-05. Prequalified Connections for Special and Intermediate Steel Moment Frames for Seismic Applications. American Institute of Steel Constructions, Chicago (IL).
[3] AISC, ANSI/AISC 360-05. Specification for Structural Steel Buildings. American Institute of Steel Construction, Chicago (IL).
[4] AISC, Steel Design Guide 20. 2007. Steel Plate Shear Walls. American Institute of Steel Constructions.
[5] Alipour M, Rahai A.R. 2011. Behavior and characteristics of innovative composite plate shear walls. Procedia Engineering, 14: 3205-3212.
[6] Alipour M, Rahai A.R. 2011. Perforated steel shear walls with FRP reinforcement of opening edges. Australian Journal of Basic and Applied Sciences, 5(10): 672-684.
[7] Behbahanifard M.R, Grondin G.Y, Elwi A.E. 2003. Experimental and numerical investigation of steel plate shear wall. Structural Engineering Reports No.254, Dept. of Civil and Environmental Engineering, University of Alberta
[8] Berman J.W, Bruneau M. 2003. Plastic analysis and design of steel plate shear walls. Journal of Structural Engineering, ASCE, 129(11), 1148-1156.
[9] Bhowmick A.K. 2009. Seismic analysis and design of steel plate shear walls. PhD thesis, Dept. of Civil and Environmental Engineering, University of Alberta, Edmonton, Alberta.
[10] CSA, CAN/CSA-S16-01. Approved June 2003. Limit States Design of Steel Structures. Canadian Standards Association, Toronto (ON).
[11] Kharrazi M, Prion H, Ventura C. 2008. Implementation of M-PFI method in design of steel plate walls. Journal of Constructional Steel Research, 64(08), 465-479.
[12] Roberts T.M, Sabouri-Ghomi S. 1991. Hysteresis characteristics of unstiffened plate shear panels. Thin-Walled Structures, 12, 145-162.
[13] Roberts T.M, Sabouri-Ghomi S. 1992. Hysteresis characteristics of unstiffened perforated steel plate shear wall. Thin-walled Structures, 14, 139-151.
[14] Thorburn L.J, Kulak G.l, Montgomery C.J. 1983. Analysis of steel plate shear walls. Structural Engineering Report No.107. Dept. of Civil Engineering, University of Alberta, Edmonton, Alberta
[15] Timler P.A, Kulak G.L. 1983. Experimental study of steel plate shear walls. Structural Engineering Report No.114. Dept. of Civil Engineering, University of

Alberta, Edmonton, Alberta.
[16] Tromposch E.W, Kulak G.L. 1987. Cyclic and static behavior of thin panel steel plate shear walls. Structural Engineering Report No.145, Dept. of Civil Engineering, University of Alberta, Edmonton, Alberta.
[17] Elgaaly, M, Hamilton, R.W.and Seshardi, (1996) Shear strengh of beams with corrugated webs, ASCE
[18] Caccese,V. and Elgaaly, M. and Chen,R. 1993. Experimental study of, thin steel plate shear walls under cyclic load. Struct.Eng., Vol.119,No.2.
[19] Driver, R.G. and Kulak, G.L. Kennedy, D.J.L. and Elwi, A.E. 1996 .siesmic performance of steel plate sheer walls based on a large scale multi story test. 11WCEE. Alcapulo Mexico
[20] Purba R. 2006. Design recommendations for perforated steel plate shear walls. M.Sc Thesis, State Univ. of New York at Buffalo, Buffalo, N.Y.
[21] Vian D, Bruneau M, Tsai K.C, Lin Y.-C. 2009. Special perforated steel plate shear walls with reduced beam section anchor beams, I: Experimental investigation. ASCE, 211-220.

.

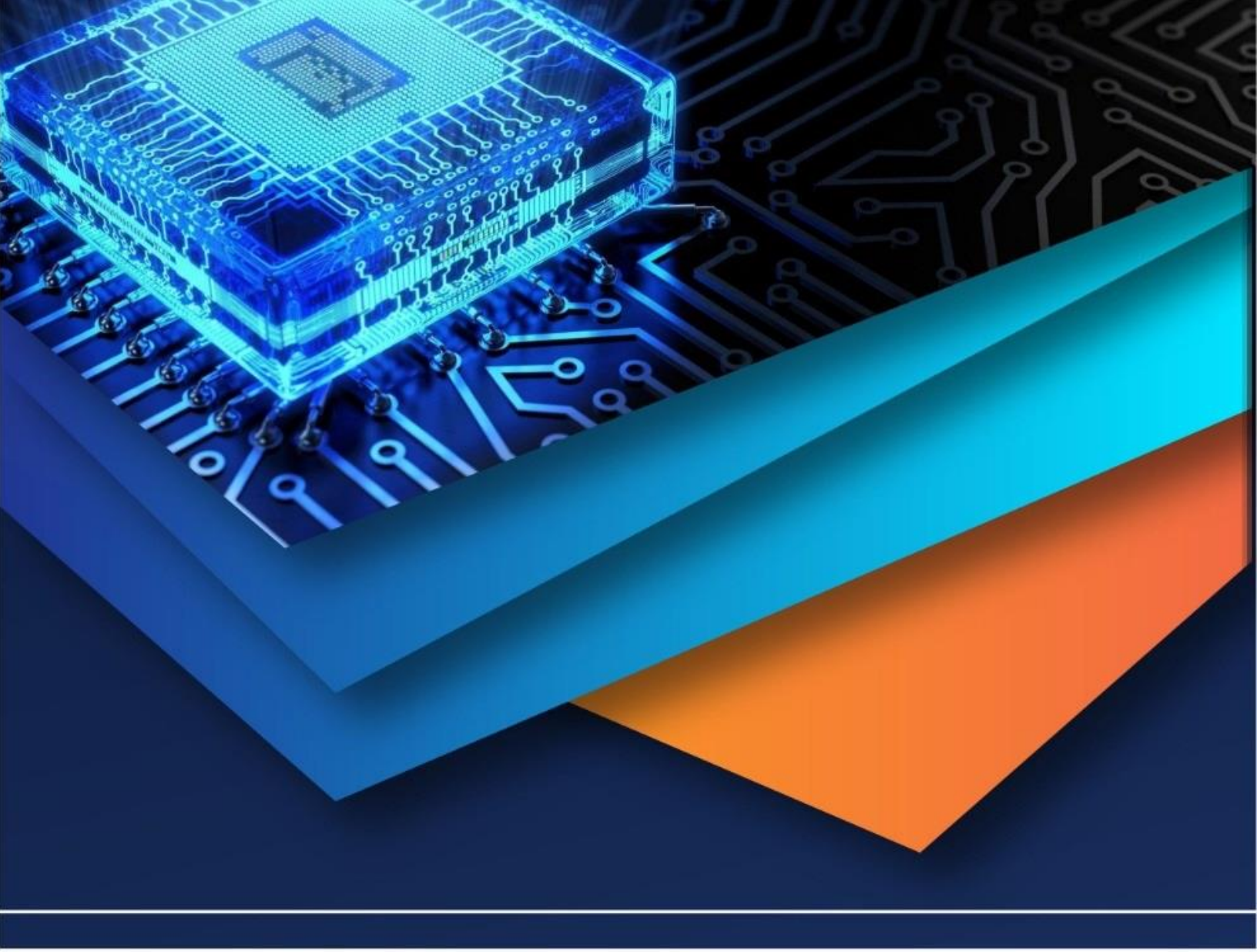

10.22214/IJRASET

45.98

IMPACT FACTOR: 7.129

IMPACT FACTOR: 7.429

INTERNATIONAL JOURNAL FOR RESEARCH

IN APPLIED SCIENCE & ENGINEERING TECHNOLOGY